ELSEVIER

Journal of Nuclear Materials 255 (1998) 153–164

journal of nuclear materials

Isotopic effects in hydrocarbon formation due to low-energy H^+/D^+ impact on graphite

B.V. Mech, A.A. Haasz *, J.W. Davis

Fusion Research Group, University of Toronto Institute for Aerospace Studies, 4925 Dufferin St., Toronto, Ontario, Canada, M3H 5T6

Received 23 September 1997; accepted 2 February 1998

Abstract

Recent developments with gaseous divertors in tokamaks have led to prospects of less energetic ion bombardment (10's of eV) of material surfaces in the divertor region. The present experiments were undertaken with the objective of studying hydrocarbon formation due to H^+/D^+ impact on graphite for energies extending down to the 10 eV range. Mass spectrometry in the residual gas was used to measure the hydrocarbon formation rates as a function of pyrolytic graphite temperature (300–1000 K) and ion energy (10–200 eV/H or D) for mass-analysed H_3^+ and D_2^+ beams (10^{18} $H^+(D^+)/m^2$ s) providing a unique opportunity to also investigate isotopic effects. The results indicate that, as the ion impact energy is reduced, a reduction in the maximum chemical yield (Y_m) is observed and the broadening of the temperature dependence profile for hydrocarbon formation leads to significant erosion for low-energy impact at room temperature. The room-temperature methane and total chemical yields display maxima at about 50 eV and decrease as the ion energy is further reduced. Where kinetic effects are expected to affect the erosion process, viz., low energy (< 25 eV)/near-room temperature, and higher energies (> 50 eV)/near T_m, an isotopic yield ratio, Y_D/Y_H of about 1.5–2 was measured. Under all other conditions studied, this ratio was near unity. Furthermore, it is evident that the dominating erosion mechanisms at low energies (< 100 eV) differ from those occurring for higher energy impact.

1. Introduction

Graphite and other carbon-based materials are excellent candidates for plasma-facing applications in tokamaks. Unfortunately, particle impact leads to erosion of these materials. Erosion reduces the component lifetimes, dilutes the fuel, and increases the plasma impurity level. Carbon can be eroded by both physical and chemical mechanisms. Physical sputtering, which involves the ejection of lattice carbon atoms, contributes to erosion for hydrogenic impact energies above ~ 40 eV [1] and is independent of the graphite temperature. This process has been studied extensively and several reviews are available [2,3]. For temperatures exceeding ~ 1200 K, radiation enhanced sublimation (RES), which also involves the displacement of carbon lattice atoms due to energetic particle impact, starts to dominate. In the case of RES, displaced carbon atoms diffuse to the surface from where they can be thermally released, leading to an erosion yield which increases monotonically with temperature [3]. In addition to physical sputtering and RES, there exists a mechanism whereby, under hydrogenic impact, hydrocarbon formation occurs in graphite and the thermally enhanced release of these hydrocarbons leads to erosion yields which, under some conditions, can be significantly greater than physical sputtering [4]. This process is called chemical erosion.

The chemical erosion characteristics of graphite have been extensively studied for energetic impact (100 eV–3 keV) in laboratory experiments. Recent reviews of these results are available [4,5]. Current divertor technology, however, has led to significantly reduced impact energies in the range of 10's of eV. Difficulties in producing relatively intense low-energy beams have resulted in com-

* Corresponding author.

0022-3115/98/$19.00
PII: S0022-3115(98)00035-X

paratively fewer laboratory investigations into the chemical erosion of graphite for ion impact below 100 eV. The limited results show, however, that the chemical erosion yield is not dramatically suppressed even for ion energies below the threshold for physical sputtering [6–10]. Using a mass-analyzed ion gun and an electrostatic lens specially designed for low energy operation (down to ~ 10 eV), we have undertaken a study of the chemical formation of hydrocarbons produced by hydrogenic impact of carbon, as a function of impact energy, carbon temperature and hydrogenic species. In two earlier papers, we have presented results on CD_4 production during 20–400 eV D_2^+ (i.e., 10–200 eV/D^+) impact on graphite [9], and CH_4, C_2H_x and C_3H_y hydrocarbon production during 30–600 eV H_3^+ (i.e., 10–200 eV H^+) impact on graphite [10]. (We note that we identify the impacting species as D^+ and H^+ even though the ionic charge is associated with the D_2^+ and H_3^+ molecular ions.) Comparison of these studies with other low-energy results [7,8] has lead to some large discrepancies, particularly with respect to the isotopic differences in the H^+ and D^+ induced erosion yields. In the present study, we have directly compared the two isotopes using improved diagnostic sensitivity and calibration capabilities. As an extension of this work, a model based on atomistic mechanisms has also been formulated [11].

2. Experiment

2.1. Experimental facility

2.1.1. Ultrahigh vacuum (UHV) system

All experiments were performed in an ultra-high vacuum facility pumped by a 360 l/s Leybold turbomolecular pump. A schematic diagram of the experimental facility is shown in Fig. 1. After atmospheric exposure, the entire UHV facility was baked at ~ 500 K for at least 24 h. If water levels remained high, a 'hot' (~ 1800 K) tungsten ring filament, producing thermal H°(D°)-atoms via contact dissociation of $H_2(D_2)$ molecules in a hydrogen backfill of 10^{-4} Torr, was operated for a further 24 h. The H° atoms, via chemical reactions with wall impurities, led to a subsequent reduction of the gaseous impurities in the residual gas. The pressure was monitored by Bayard–Alpert type ionization gauges and the system routinely achieved ultimate pressures of $< 5 \times 10^{-10}$ Torr consisting mainly of H_2 and CO, with much smaller contributions from H_2O and CO_2.

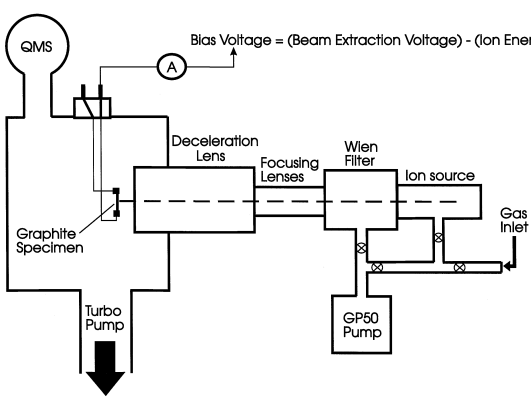

Fig. 1. Schematic diagram of the experimental facility. Ions produced in the source are extracted and transmitted through the Wien filter and electrostatic deceleration lens. The ion beam impacts the graphite specimen at normal incidence and the hydrocarbon products are detected in the residual gas using a quadrupole mass spectrometer (QMS).

2.1.2. Mass-analyzed ion gun

An electron-impact extraction type ion source (SPECS IQE 12/38) was used to produce fairly intense hydrogenic (H_3^+ and D_2^+) ion beams. A differentially-pumped Wien-type velocity filter (SPECS), installed after the focusing stage of the ion source, ensured that the transmitted ions were mass selected. The ion source and filter together imposed limits on the useable energy ranges for both protium (400 to 700 eV H_3^+) and deuterium (900 to 1300 eV D_2^+). It was not possible to obtain H^+, H_2^+, D^+ or D_3^+ beams with sufficient beam current to conduct experiments. Unfortunately, these energy ranges were still too high to perform low-energy erosion experiments, characteristic of the divertor region of a tokamak, and so it was necessary to decelerate the beam.

When working with intense ion beams, it is often difficult to simply decelerate the beam at the target since space-charge effects lead to rapid expansion of the beam and a subsequent loss of current density. A common approach used to overcome this problem is to transmit the beam through an electrostatic lens in order to focus the ions against space-charge forces.

In the present experiments, a five-element electrostatic lens was designed and installed between the Wien filter and the graphite specimen. A single-pin probe was used to profile the transmitted beam in order to optimize the applied lens element potentials. A small flux of electrons, presumably secondaries produced in the lens, was also measured on the specimen, producing a small negative offset to the beam profiles. In the case of deuterium, it was found that the lens could transmit 100% of the filtered beam at final energies of 200 eV/atom, and 80% of the filtered beam for final energies of 10 eV/atom. The beam exhibited a Gaussian profile resulting in spot sizes of 3–4 mm in diameter. Similar results were obtained for protium. The obtainable current densities were $1–3 \times 10^{18}$ $H^+(D^+)/m^2$ s.

2.1.3. Graphite specimen

A single graphite specimen (as-deposited pyrolytic graphite, HPG99, manufactured by Union Carbide) was

used for all of the experiments. This polycrystalline graphite exhibits both micro and macro porosity, has a mosaic spread of $\sim 30°$, and a density of 2200 kg/m^3. Temperature variation of the graphite specimen was achieved by resistive heating, and the temperature was monitored by an optical pyrometer which was calibrated against a type-C tungsten–rhenium thermocouple. Following exposure to air, the specimen was baked at 1100 K for 12 h. Annealing at ~ 2000 K for 30 s was performed between experiments where the ion energy was changed, in order to remove radiation-induced damage [12].

2.2. Experimental procedure

The graphite specimen was located 50 mm downstream of the electrostatic deceleration lens. The mass-selected beams of D_2^+ and H_3^+ ions impacted on the specimen at normal incidence. When these low-energy molecular ions break up, upon striking the graphite surface, there may be an uneven sharing of the energy between the atoms, on the order of the molecular binding energy, a few eV. It is also possible that the atoms in the molecular ion do not act independently in the near-surface region and this may affect the hydrocarbon formation process. The fact that different molecular ions have been used for H and D may also have an effect. The beam intensity was measured on the specimen and small corrections were made for the contributions of secondary electrons originating in the deceleration lens which reached the specimen. These corrections were based on the beam profiles discussed in Section 2.1.2. As well, secondary electron emission from the specimen was suppressed by the high voltage applied to the specimen (typically > 200 V higher than the last lens electrode). Ion fluxes of $\sim 1 \times 10^{18}$ $H^+(D^+)/m^2$ s were used in all of the experiments discussed below. There was no evidence of beam divergence at low energies to suggest an electrically insulating layer was being formed on the graphite surface due to the low energy ion implantation.

It should be noted that electron-impact ion sources of the type used in the present experiments have energy spreads of < 1eV [13] and so the decelerated beam was not energy analyzed. An error of ± 5 eV is estimated for the energy of the H_3^+ and D_2^+ molecular ions due to difficulties in measuring the specimen bias potential. This implies energy uncertainties of ± 1.7 and ± 2.5 eV for the H^+ and D^+, respectively. An upper limit of the neutral content of the beam can be obtained from an estimate of the fraction of the beam undergoing charge exchange in the lens: $\sim 6.5 \times 10^{-4}$. In fact, only a small percentage of this number is expected to impact the specimen. Measurements, based on D retention, have placed an upper limit on the neutral fraction striking the target at 10^{-4}. This should make the synergistic contribution from energetic particles negligible [14].

2.2.1. Residual gas analysis

All reaction products were monitored in the residual gas using an Extranuclear quadrupole mass spectrometer (QMS) in the test chamber. Care was taken to ensure that the background hydrogen pressure (which has been found to affect the quadrupole sensitivity) was kept nearly constant during the erosion experiments. The sensitivity of the QMS was calibrated in situ against known leaks of $CH(D)_4$, $C_2H(D)_4$, and $C_3H(D)_6$. The sensitivities for the other reaction products ($C_2H(D)_2$, $C_2H(D)_6$ and $C_3H(D)_8$), as well as their cracking patterns, were inferred using a combination of leak bottles and previous calibrations of a similar QMS [14].

Data acquisition was accomplished using a National Instruments ATMIO16 board and the LabWindows user interface environment. The erosion product spectrum analysis was accomplished using a matrix analysis technique described elsewhere [14].

2.2.2. Wall contribution to the erosion signals

In general, a fraction of the hydrogen ions incident on graphite are reflected from the specimen to the walls of the vacuum chamber where they can form hydrocarbons which may subsequently be desorbed and detected by RGA. This may be called the wall contribution to the erosion signal and should be subtracted from the detected QMS signals to obtain the true chemical erosion yields. In practice, it is not always necessary to make this correction since, for high energy H^+, D^+ impact, the reflection coefficient is small [15] and the chemical erosion yield of graphite is high, so the wall contribution to the total signal is negligible. In the present experiments, however, the opposite is true. For low incident ion energies, the reflection coefficient is relatively higher [15] and the erosion signals are relatively lower so that the wall contribution may actually dominate the measured signal. It becomes necessary then to quantify and subtract the wall contribution in order to obtain the true erosion yields.

In the present experiments, the wall contribution was determined in the following manner. The graphite specimen was annealed at 1200 K for ~ 10 s, in order to thermally desorb the hydrogen in the specimen, and then allowed to cool to room temperature. The ion beam was then turned on and a fast rise was observed in the hydrocarbon signals, with a time constant of ~ 3 s, followed by a long slower increase with an energy-dependent time constant of ~ 20–100 s. Now, for the energetic hydrogen impact on graphite, there is essentially 100% retention of the non-reflected particles until a fluence corresponding to the saturation of the implantation zone is reached [16,17]. Thus, immediately after the beam is turned on, the graphite specimen is not hydrogenated and the initial steep rise cannot be due to hydrocarbons originating from the specimen. There is, however, an abundance of hydrocarbon precursors found on the vacuum chamber walls due to the history of particle bombardment resulting in carbon sput-

tering, and this initial steep rise can be attributed to hydrocarbon formation resulting from the interaction of the reflected hydrogen with the walls. The subsequent long steady signal increase is due to hydrocarbons originating from the specimen as its hydrogen inventory approaches steady state. Within experimental error, the measured wall contribution was found to be independent of the graphite specimen temperature. It was not, however, independent of

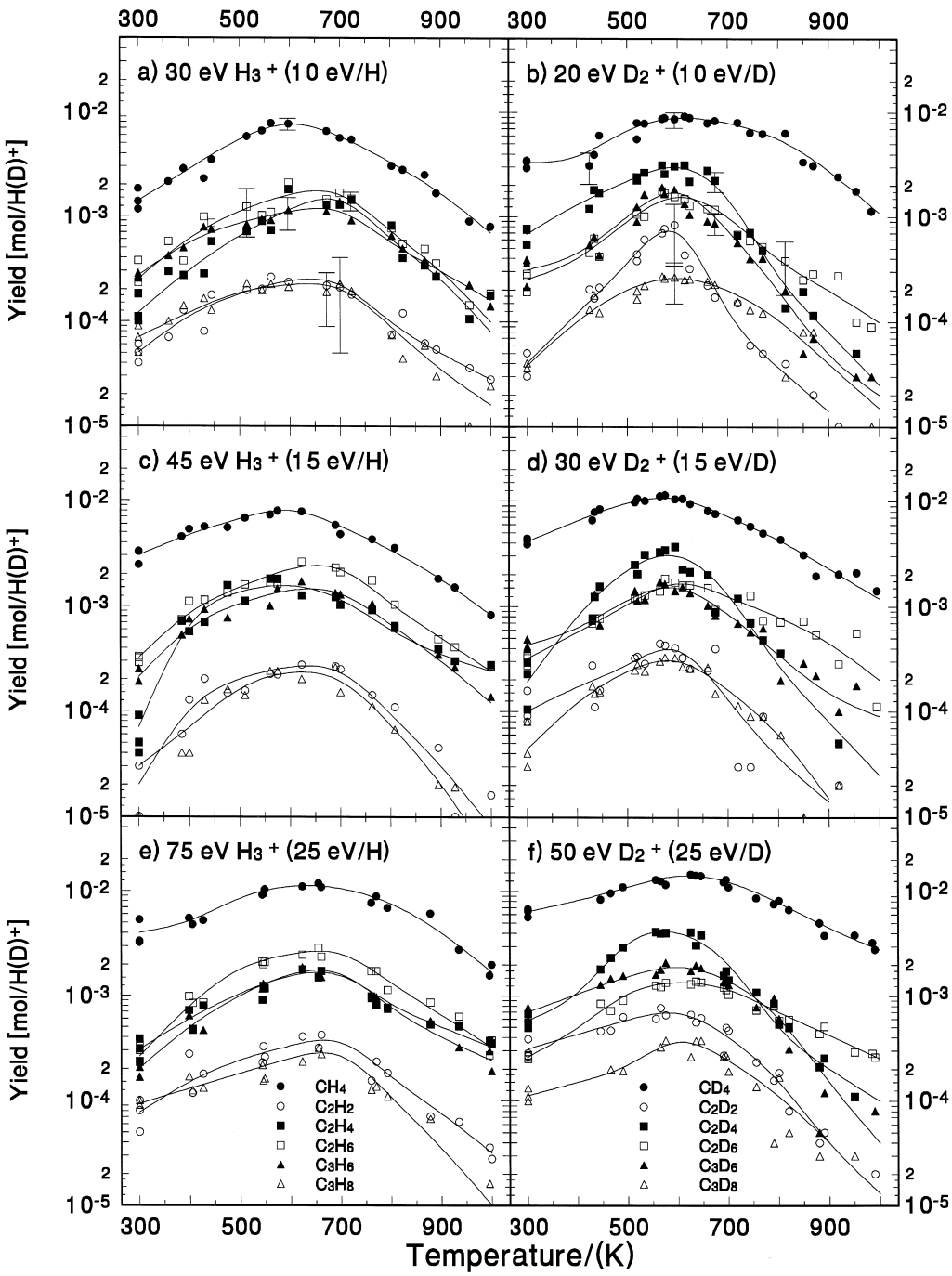

Fig. 2. Hydrocarbon yields as a function of temperature for H^+ (a,c,e), and D^+ (b,d,f) impact at energies of 10, 15, and 25 eV/atom. The lines through the data serve to aid the reader.

ion energy; the background contribution to the measured signal was ~30% for 200 eV impact, and ~75% for 10 eV impact. It should be noted that where the calculated yields are small ($< 10^{-3}$ molecule/H(D)) small errors in calculating the wall contribution may lead to large relative errors in the reported yields.

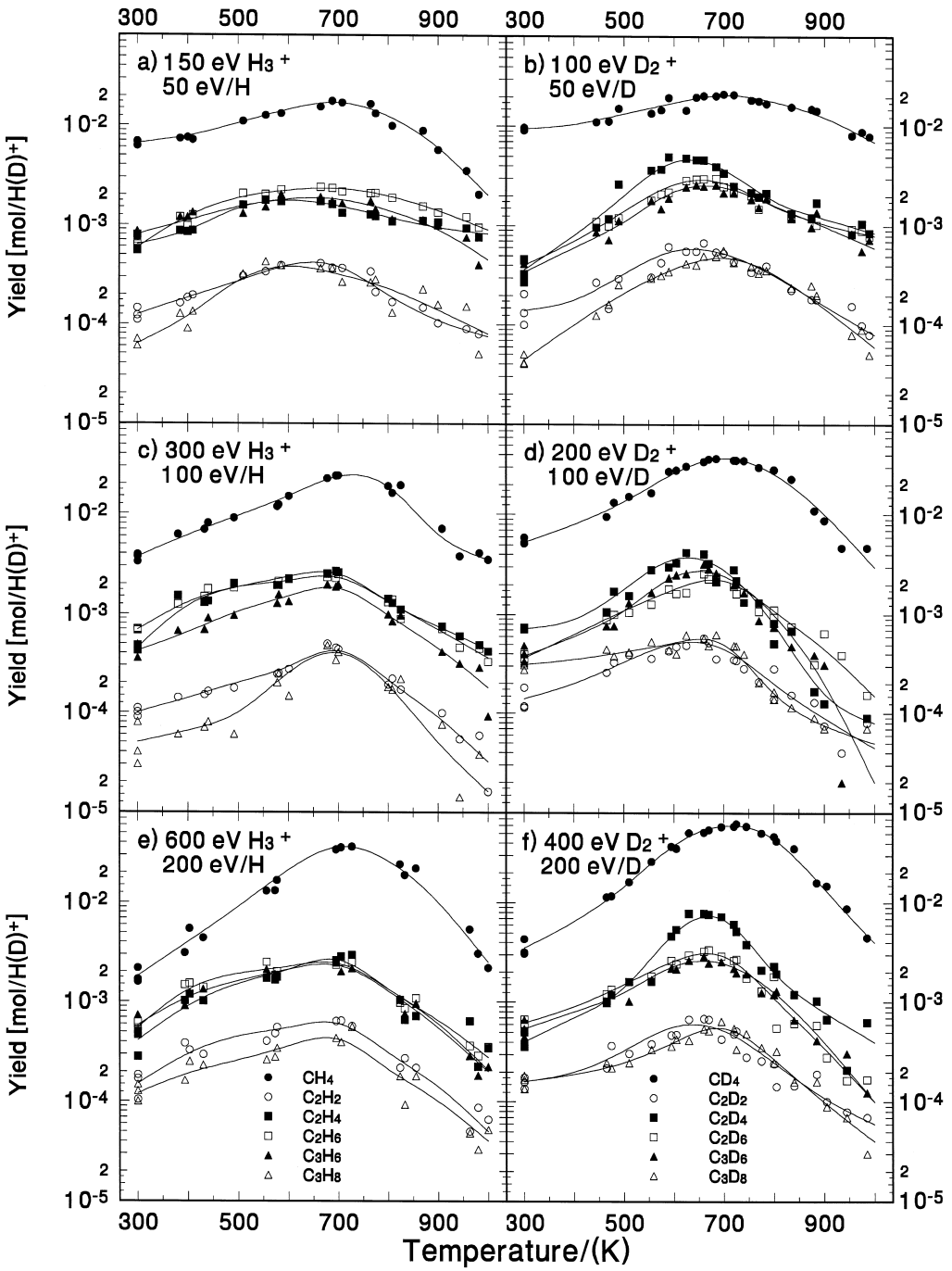

Fig. 3. Hydrocarbon yields as a function of temperature for H^+ (a,c,e), and D^+ (b,d,f) impact at energies of 50, 100, and 200 eV/atom. The lines through the data serve to aid the reader.

3. Experimental results

Chemical erosion experiments were conducted for H^+ and D^+ impact at six energies (10, 15, 25, 50, 100, and 200 eV/atom) and the hydrocarbon spectra, as a function of the graphite temperature, are presented in Figs. 2 and 3. From these figures, it is clear that methane is the predominant erosion product regardless of the impacting isotope, ion energy, or graphite temperature. In general, the $C_2H(D)_2$ and $C_3H(D)_8$ molecular yields are the smallest, while the remaining heavier hydrocarbon yields are roughly equal. Of course, one must consider the number of carbon atoms in the molecular species when determining their relative contribution to the total chemical erosion yield.

The presentation and discussion of the experimental results will cover the temperature dependence of the methane and total chemical erosion yields, the energy dependence of the methane, heavier hydrocarbon, and total chemical erosion yields for both H and D. Also provided are isotopic comparisons of the chemical erosion yields as a function of energy for the total chemical yields. Finally, the present data are compared with previously published low-energy results.

3.1. Temperature dependence

In Fig. 4a, the methane yield due to H^+ impact is shown as a function of temperature for each of the 6 impact energies. Similar results for D^+ impact are presented in Fig. 4b. In general, we observe that the temperature profiles are more peaked at the higher energies and there is a strong dependence in the peak yield (Y_m) on ion energy. For H^+ impact at 200 eV, $Y_m \sim 0.036$ CH_4/H^+, and this is reduced to $\sim 7.7 \times 10^{-3}$ CH_4/H^+ at 10 eV. The corresponding values for D^+ impact are $Y_m \sim 0.061$ CD_4/D^+ at 200 eV, and $\sim 8.9 \times 10^{-3}$ CD_4/D^+ at 10 eV.

Similar observations can be made for Fig. 4c,d where the total chemical yields are shown for H^+ and D^+ impact. In the case of protium impact (Fig. 4c), the maximum yield is reduced from ~ 0.056 C/H^+ at 200 eV to ~ 0.018 C/H^+ at 10 eV. For deuterium impact (Fig. 4d), the maximum chemical yields are ~ 0.089 C/D^+ and ~ 0.023 C/D^+ at 200 eV and 10 eV, respectively.

The increase in the maximum methane and total chemical yields with increasing impact energy indicates the possible role that damage deposition, in the form of broken

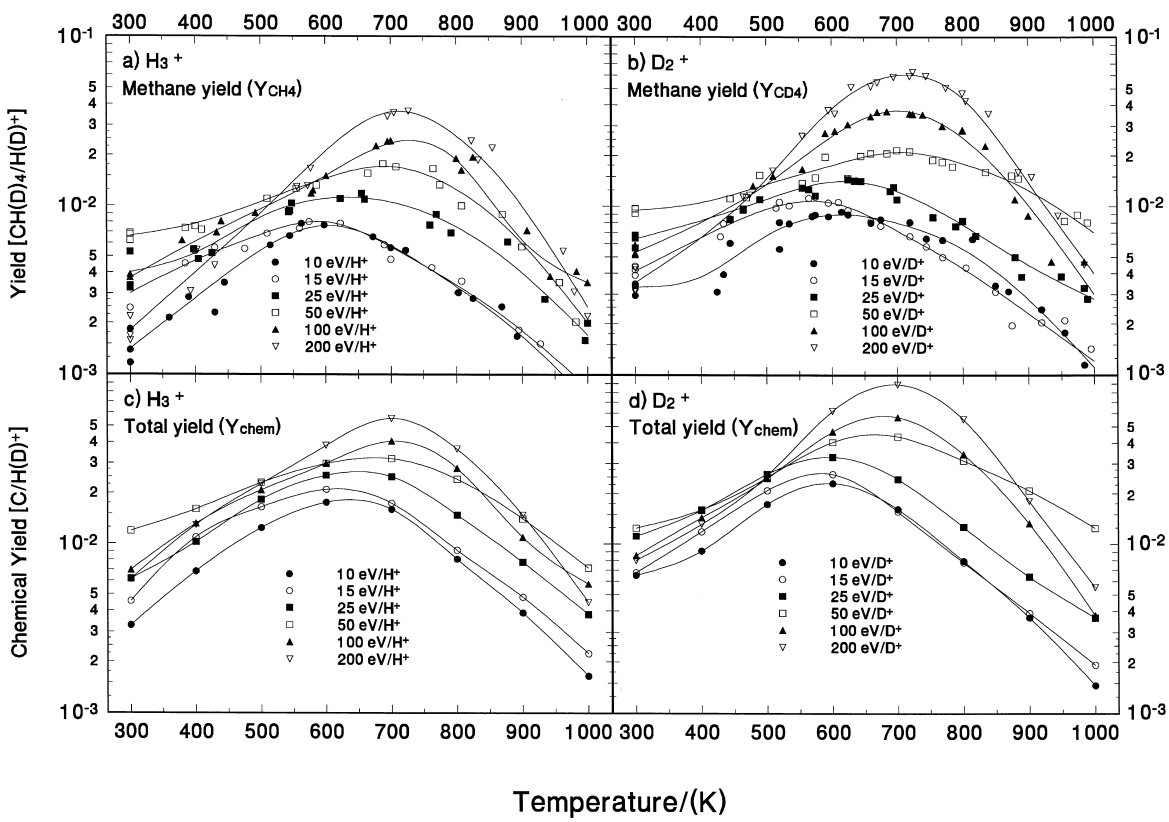

Fig. 4. Methane (a,b), and total chemical erosion (c,d) yields, as a function of specimen temperature for 6 selected ion impact energies. For all figures in this paper, Y_{chem} is the total number of C-atoms detected divided by the incident flux, i.e., $Y_{chem} = ((CH_4 + 2x(C_2H_2 + C_2H_4 + C_2H_6) + 3x(C_3H_6 + C_3H_8))/(H)$, with a similar expression for D. The lines through the data serve to aid the reader.

carbon–carbon bonds, plays in increasing the concentration of hydrocarbon groups attached to the graphitic network in the near-surface region. The thermally activated release of these groups is thus enhanced at higher temperatures.

We also note in Fig. 4 that the temperature at which the maximum yield occurs, T_m, increases with increasing ion energy. This suggests that the thermal release of hydrogen, which serves to reduce the hydrocarbon yield at higher temperatures, is delayed by kinetic processes associated with the energetic particles. This shift in T_m has been noted in previous low-flux ($< 5 \times 10^{18}/m^2$ s) erosion experiments [6,14], but not when higher fluxes were used [7,8,18,19], suggesting that there is a saturation effect in this process.

3.2. Energy dependence

The energy dependence of the methane, heavier hydrocarbons, and total chemical erosion yields at four selected temperatures for both H^+ and D^+ impact is shown in Fig. 5. Key features of this figure are noted below.

(1) At room temperature (Fig. 5a,b), we note that the methane yield exhibits a shallow maximum near 50 eV for

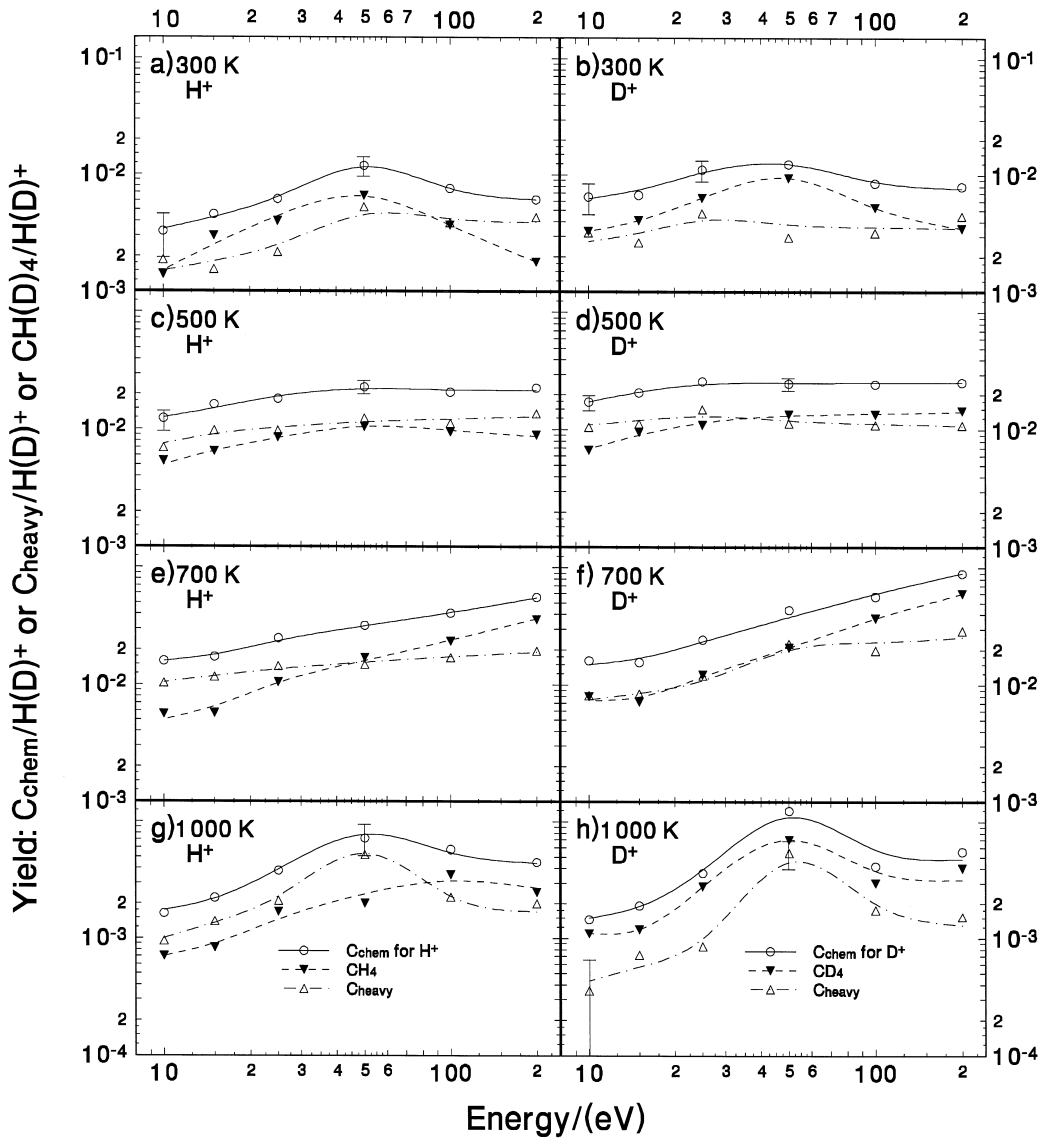

Fig. 5. Methane, heavy hydrocarbon, and total chemical erosion yields as a function of incident particle energy for H^+ (a,c,e,g), and D^+ (b,d,f,h) impact at four selected specimen temperatures. The heavy hydrocarbon yield, $Y_{heavy} = [C_{heavy}]/[H(D)^+]$, is the difference between the total chemical yield and the methane yield. The lines through the data serve to aid the reader.

both H^+ and D^+ impact, where the methane yield values are $\sim 6.6 \times 10^{-3}$ CH_4/H^+ and $\sim 9.5 \times 10^{-3}$ CD_4/D^+, respectively. At these low temperatures, it is unlikely that thermal release of methane plays a role in the observed yield. Instead, this behaviour is consistent with the process of kinetic ejection of weakly bound surface methyl ligands hypothesized by Roth and García-Rosales [20]. As the ion energy is increased from 10 eV, one might expect an increase in the rate of kinetic ejection as more energy is transferred to these surface methyl groups. As the ion energy is further increased, however, it seems likely that implantation of the ions reduces their interaction with these surface groups.

If we consider the heavier hydrocarbon production at room temperature, we observe that the yields are only moderately dependent on the impacting energy suggesting an additional release mechanism which relies on some sort of electronic or lattice excitation process. The nature of this release mechanism is unknown at this time. (TRVMC ion–surface interaction calculations [21] for 10–25 eV H^+/D^+ impact on carbon indicate an approximate equal sharing of incident ion energy between electron energy loss and phonon excitation; at this energy, no nuclear damage occurs.)

The total chemical erosion yields at room temperature exhibit essentially the same behaviour as that of methane alone, only moderated by the heavier hydrocarbon contributions which are less dependent on impact energy. This general trend is also observed at the other temperatures studied.

(2) For impact at 500 K (Fig. 5c,d), we note that, within experimental error, the methane and heavy hydrocarbon yields are virtually coincident and relatively independent of energy over the range studied here. Consequently, the total chemical erosion yield is nearly a constant at this temperature.

(3) For temperatures near the peak for the methane yield due to energetic impact, 700 K (Fig. 5e,f), we observe an increase in the methane yield between 10 and 200 eV which approaches an order of magnitude. Presumably, kinetic ejection of surface groups may still occur, but it is the thermal release of methane which is dominating the observed yield. Clearly then, kinetic processes associated with the energetic ions, including damage deposition, lead to the enhanced methane yield. These processes and others are discussed more fully in [11]. If we consider the heavier hydrocarbon yields, we note that the increase between 10 and 200 eV is much less dramatic. This raises a few possibilities; (i) the thermal release rate for these ligands is smaller, (ii) the heavy hydrocarbon groups produced at greater depths are broken up as they move to the surface [22,23], or (iii) the kinetic effects of the energetic ions lead to preferential formation of methyl groups in the implantation zone.

For $H^+(D^+)$ impact at 700 K, we also note that heavy hydrocarbons become more important as the ion energy is reduced. In the case of H^+ impact (Fig. 5e), heavy hydrocarbons account for $\sim 35\%$ of the total chemical yield at 200 eV, and this increases to $\sim 50\%$ at 50 eV and $\sim 70\%$ at 10 eV. For D^+ impact (Fig. 5f), the heavy hydrocarbon yield again accounts for $\sim 30\%$ of the total yield at 200 eV and $\sim 50\%$ for all energies ≤ 50 eV. The slight difference between the isotopes for energies below 50 eV falls within experimental errors. Similar hydrocarbon ratios have been noted previously [7,14,24,25].

(4) For $H^+(D^+)$ impact proceeding at 1000 K (Fig. 5g,h), thermal release of hydrogen results in reduced chemical yields (note change in scale). The yields exhibit a peak near 50 eV. Since we would expect kinetic ejection to be negligible at these high temperatures [11,20], this local maximum suggests a possible correlation between the distributions of both the ions and the damage they deposit. For ion energies producing the greatest overlap of these distributions, significant heavy hydrocarbon formation and release may still be possible, even at 1000 K. The trends

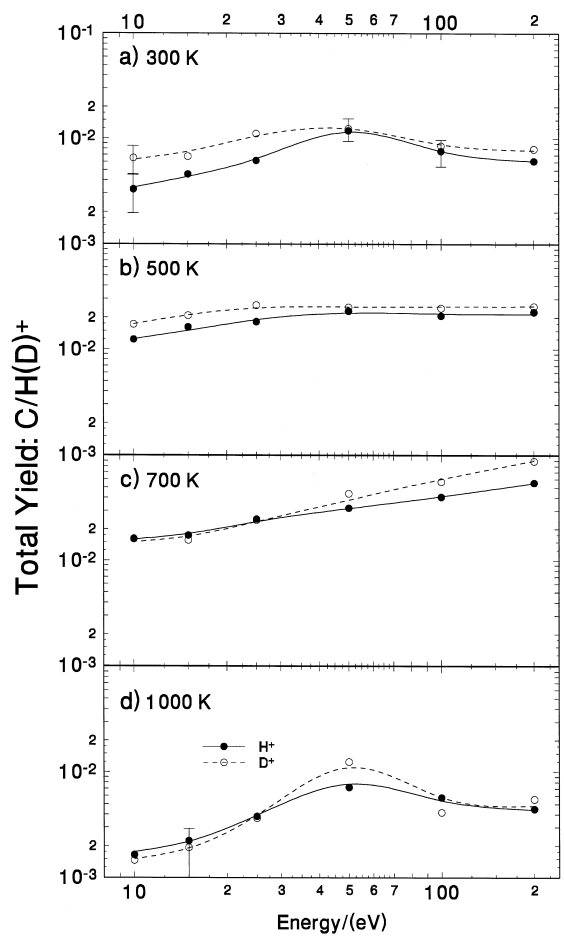

Fig. 6. Isotopic comparison of the total chemical erosion yields, as a function of impact energy, due to H^+ and D^+ impact at four selected specimen temperatures.

for H^+, where the heavy hydrocarbon production exceeds that of methane between 10 and 80 eV, and D^+, where methane dominates for all energies (10 to 200 eV), is puzzling. Given the larger relative errors in this region, the observed differences may not be significant.

3.3. Isotopic effects in the chemical erosion of graphite

In the present experiments, we have a unique opportunity to determine the isotopic effect on the chemical erosion yield of graphite over a range of impact energies and specimen temperatures. Here, we will discuss the isotopic effect on the total chemical erosion yields.

In Fig. 6, the total chemical yield is plotted as a function of $H^+(D^+)$ energy for four selected temperatures. We note that, over most of the energy/temperature range explored, the isotopic effect is small. We observe only two regions where the isotopic effect approaches or falls outside the limits imposed by experimental uncertainties. Namely, low energy (< 25 eV) impact at room temperature and higher energy (> 50 eV) impact near T_m.

Since the chemistry of the two isotopes is essentially the same, we expect isotopic differences to arise from kinetic effects. For room-temperature impact (Fig. 6a), hydrocarbon production is likely to be due to kinetic ejection of weakly bound surface hydrocarbons. This is especially true for low-energy impact below the threshold for physical sputtering. For such collisional phenomena, we expect that the heavier deuterium ions would be more efficient at transferring their energy to hydrocarbon ligands. If we consider the simple case of an elastic binary head-on collision between the impacting isotope and the corresponding methyl group, we determine that a deuterium ion would transfer 36% of its energy, while a protium ion would transfer 23.4% of its energy to the methyl radical. The ratio of energy transfer due to D vs. H is ~ 1.5. Thus, it seems reasonable to expect an isotopic effect in this low-energy and low temperature regime. The experimental measurements are consistent with this expected effect. Ion implantation negates this effect at higher energies.

For impact proceeding near $T_m \sim 700$ K (Fig. 6c), thermal release of hydrocarbons dominates the erosion yield. Thus, any kinetic effects on the concentration of hydrocarbon ligands in the implantation zone should appear as isotopic effects. The most obvious of these is damage deposition in the form of broken carbon–carbon bonds, which serves to increase the concentration of hydrocarbon ligands in the implantation zone. We expect that deuterium would deposit more damage than protium and

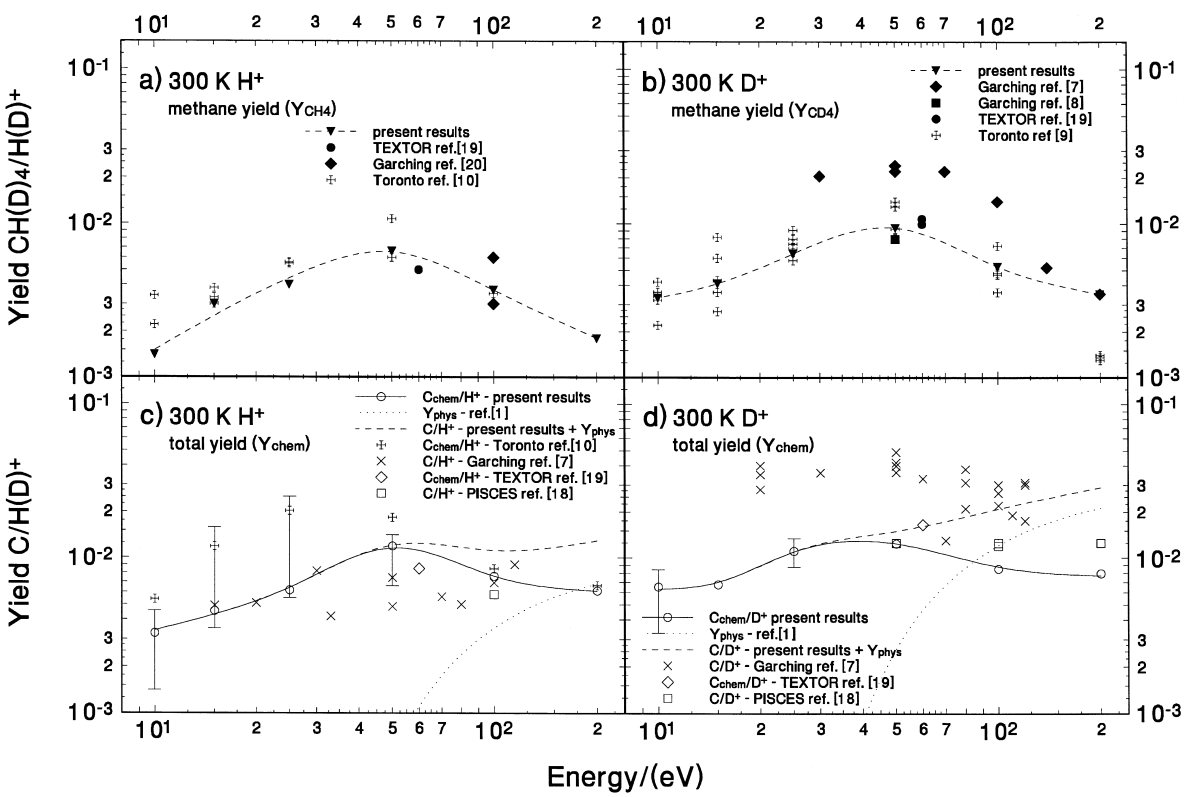

Fig. 7. Comparison of the present experimental data at 300 K, for methane (a,b), and total chemical erosion (c,d) yields due to $H^+(D^+)$ impact on graphite, with previous ion-beam [7–10,20] and higher flux density plasma-device [18,19] results.

this would explain the isotopic effect observed for higher energy impact at 700 K. For low-energy impact, damage deposition is not a factor and since thermal release dominates over kinetic ejection at this temperature (T_m), there is no isotopic effect observed.

In general, we conclude that the isotopic effect in the total chemical yield is about 1.5–2 for the low-energy (< 25 eV)/near-room temperature and higher energy (> 50 eV)/near T_m cases, where kinetic effects are expected to affect the erosion process. For the remaining cases studied, no isotopic effects were observed.

3.4. Comparison with previously published data

3.4.1. At room temperature

In Fig. 7, we compare the present results with previously published low-energy methane and total chemical erosion yield data, for impact proceeding at room temperature.

If we consider the methane yields due to H^+ impact (Fig. 7a), we observe that the TEXTOR Sniffer Probe experiment [19] and previous ion-beam results [10,20] show very good agreement with the present data. If we consider D^+ impact (Fig. 7b), however, we note that, while there is good agreement between the present data and most previous results [8,9,19], the methane yields determined by Roth and Bohdansky [7] are higher by up to a factor of ~ 3 or more than the present yields.

When discussing the total yields, we must distinguish between the total chemical yields and the total erosion yields. Experiments using mass loss measurements provide the total sputtering (chemical + physical) yield so we have to add the physical sputtering contribution to the present results in order to effect a comparison. Other experiments using RGA or LOS measure the total chemical erosion yields, hence, both the total chemical and the total sputtering (chemical + physical) yield curves are shown in Fig. 7c,d.

If we consider the total chemical erosion yield due to H^+ impact (Fig. 7c), we note again that the TEXTOR result [19] shows good agreement. Our previous ion-beam data [10] using a similar experimental setup, but with a different quadrupole, are higher by a factor of 3–4 in the energy range of 15 to 25 eV, but agree well elsewhere. After careful consideration of the potential errors associated with the small C_2H_x and C_3H_y signals in these previous experiments, we feel that it is more appropriate to extend the lower ends of these room-temperature error bars down to the methane yield values. In the present experiments, a more accurate quadrupole was used to alleviate some of these difficulties. The total (chemical + physical) yields measured in PISCES [18] and by Roth and Bohdansky [7] are a factor of 1.5 to 2 times smaller than those observed in the present experiments. The higher fluxes used in these previous experiments may account for some of the discrepancy. (The effect of flux density on chemical

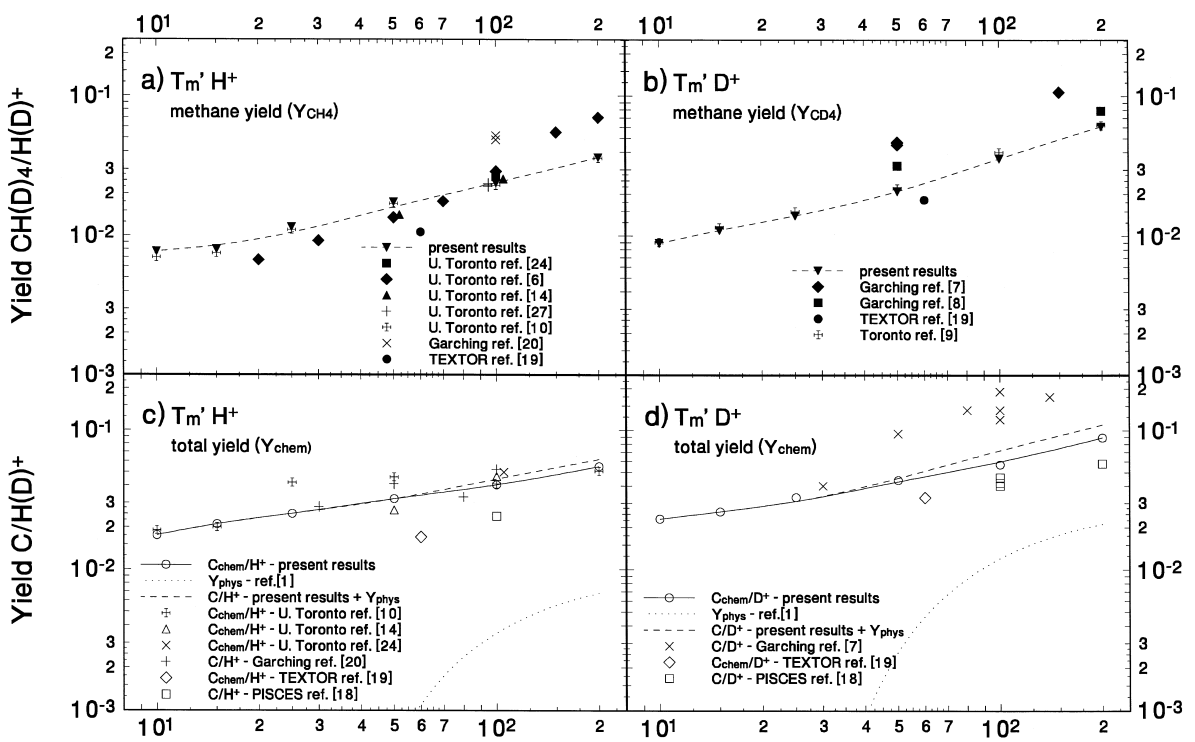

Fig. 8. A comparison of the present experimental data at T_m'', for methane (a,b), and total chemical erosion (c,d) yields due to $H^+(D^+)$ impact on graphite, with previous ion-beam [6–10,14,20,24,27] and higher flux density plasma-device [18,19] results.

erosion is uncertain, however, there may be some evidence of reduced yields at high flux density [4,26].) Also, uncertainties in determining the ion flux, energy and energy distributions in plasma experiments may account for some of the difference between the PISCES yields and our results. For D^+ impact at 300 K (Fig. 7d), the present total yield data agree well with the TEXTOR [19] results and the low-energy PISCES [18] data. The PISCES yields at higher energies are lower than the present values, corrected to include physical sputtering. Previous ion-beam data [7] agree well for impact energies above 50 eV, but are a factor of 3–4 higher than the present data at lower energies.

3.4.2. At T'_m

In Fig. 8, the methane and total yield data are shown for H^+ and D^+ impact at T'_m (T'_m = temperature corresponding to T_m in a particular experiment). If we consider the methane yields (Fig. 8a,b), we note that there is, in general, very good agreement between previous [6,8–10,14,19,20,24,27] and present results. Once again, however, the D^+ results of Roth and Bohdansky [7] (Fig. 8b) are higher by a factor of 2–2.5.

For H^+ impact at T'_m (Fig. 8c), there is strong agreement between previous ion beam data [10,14,20,24] and the present results, while the TEXTOR [19] and PISCES [18] results are a factor of ~ 2 lower. Still, considering the much higher flux ($\sim 10^{22}$ D^+/m^2 s) employed in these experiments, the agreement is good. For D^+ impact (Fig. 8d), the agreement between the present data and the high flux results obtained in plasma devices [18,19] is good. The ion-beam results of Roth and Bohdansky [7], however, are higher again by a factor of 1.7–3.

4. Conclusions

A comprehensive study of the chemical erosion of pyrolytic graphite due to low-energy H^+ and D^+ impact has been performed. Experimental measurements were made of the methane and heavier hydrocarbon erosion yields due to protium and deuterium impact in the energy range of 10 to 200 eV/$H^+(D^+)$ and graphite temperatures in the range of 300 to 1000 K, for a flux density of 10^{18} $H(D)/m^2$ s. The use of both protium and deuterium as impacting species has allowed for a systematic study of the isotopic effect on chemical erosion of pyrolytic graphite.

As the incident H^+ or D^+ energy is reduced, the methane yield as a function of graphite temperature broadens such that significant yields are observed even for impact at room temperature. Such behaviour has been noted previously [7,10]. This room temperature yield evidently depends on kinetic ejection of near surface methyl radicals and is not energy independent below 100 eV, but instead peaks for impact energies near 50 eV. For the incident H^+ and D^+ flux density used in the present experiments (10^{18} $H^+(D^+)/m^2$ s), the maximum yield (Y_m), and the temperature at which this occurs (T_m), shift downwards as the impact energy is reduced below 200 eV. The downwards shift in Y_m with decreasing ion energy has been observed in several previous experiments [6–8,14], but the shift in T_m has only been noted for relatively low incident H^+ fluxes ($< 5 \times 10^{18}$ H^+/m^2 s) [6,9,10,14].

As the graphite temperature increases above 300 K, thermally activated chemical processes become important and lead to an enhancement in the methane yield regardless of the incident particle energy. As well, for impact energies in excess of ~ 40 eV, damage deposition resulting in broken carbon–carbon bonds further enhances the methane yields at higher temperatures.

The total chemical erosion yields of pyrolytic graphite exhibit a gross behaviour which is very much like that due to methane in that the temperature dependence broadens and Y_m, and T_m shift downwards with decreasing ion energy. The contribution of the heavy hydrocarbons, which is less dependent on impact energy, tends to have a moderating effect on many of the trends observed for methane production. For plasma-facing graphite surfaces in reactors, where we desire low erosion yields, we conclude that it is more important to control graphite temperature (near 300 K or 1000 K) than it is to reduce ion energy, although there is still an advantage to lower energy impact. From an engineering standpoint, it may also be desirable to operate at a temperature of ~ 500 K where the total chemical yield is nearly independent of ion energy over the range of 10 to 200 eV.

Within experimental errors, the isotopic effect on the total chemical erosion yield is less than a factor of 2, with yields due to D^+ impact being higher for the most part. The only regimes where the isotopic effect approaches a factor of 1.5–2 are for 10 eV impact at room temperature and higher energy (> 50 eV) impact near T_m. For all other temperatures and energies the isotopic effect was not significant. These values agree reasonably well with the factor of ~ 2 observed in TEXTOR [19] and PISCES [18], but are significantly lower than the factor of ~ 5 determined by Roth and Bohdansky [7]. Based on energy transfer and damage deposition considerations, we do not expect an isotopic enhancement of greater than a factor of 2 for D^+ impact over H^+; this is consistent with our present observations.

Acknowledgements

This work was supported by the Canadian Fusion Fuels Technology Project and by the Natural Sciences and Engineering Research Council of Canada. The assistance of C.

Perez in constructing the lens is greatly appreciated. The authors also thank Dr E. Vietzke for many useful discussions.

References

[1] C. García-Rosales, W. Eckstein, J. Roth, J. Nucl. Mater. 218 (1994) 8.
[2] W. Eckstein, J. Bohdansky, J. Roth, Suppl. Nucl. Fusion 1 (1991) 51.
[3] W. Eckstein, V. Philipps, in: W.O. Hofer, J. Roth (Eds.), Physical Processes of the Interaction of Fusion Plasmas with Solids, Academic Press, 1996, p. 93.
[4] E. Vietzke, A.A. Haasz, in: W.O. Hofer, J. Roth (Eds.), Physical Processes of the Interaction of Fusion Plasmas with Solids, Academic Press, 1996, p. 135.
[5] J. Roth, E. Vietzke, A.A. Haasz, Suppl. Nucl. Fusion 1 (1991) 63.
[6] C.H. Wu, J.W. Davis, A.A. Haasz, Proc. 15th Conf. on Controlled Fusion and Plasma Heating, Dubrovnik, May 16–20, 1988, Europhysics Conf. Abstracts, Vol. 12B, Part II, p. 691.
[7] J. Roth, J. Bohdansky, Nucl. Instrum. Meth. B 23 (1987) 549.
[8] C. García-Rosales, J. Roth, J. Nucl. Mater. 196–198 (1992) 573.
[9] A.A. Haasz, B.V. Mech, J.W. Davis, J. Nucl. Mater. 231 (1996) 170.
[10] B.V. Mech, A.A. Haasz, J.W. Davis, J. Nucl. Mater. 241–243 (1997) 1147.
[11] B.V. Mech, A.A. Haasz, J.W. Davis, A model for the chemical erosion of graphite due to low-energy hydrogenic impact, J. Appl. Phys., submitted.
[12] E. Vietzke, V. Philipps, K. Flaskamp, J. Nucl. Mater. 162–164 (1989) 898.
[13] I.W. Drummond, Vacuum 34 (1984) 51.
[14] J.W. Davis, A.A. Haasz, P.C. Stangeby, J. Nucl. Mater. 155–157 (1988) 234.
[15] W. Eckstein, Suppl. Nucl. Fusion 1 (1991) 17.
[16] G. Staudenmaier et al., J. Nucl. Mater. 84 (1979) 149.
[17] R. Siegle, J. Roth, B.M.U. Scherzer, S.J. Pennycook, J. Appl. Phys. 73 (5) (1993) 2225.
[18] D.M. Goebel, J. Bohdansky, R.W. Conn et al., Fusion Tech. 15 (1988) 102.
[19] V. Philipps, E. Vietzke, M. Erdweg, J. Nucl. Mater. 162–164 (1989) 550.
[20] J. Roth, C. García-Rosales, Nucl. Fusion 36 (12) (1996) 1647.
[21] W. Eckstein, Computer Simulation of Ion-Solid Interactions, Springer Series in Material Science, Vol. 10, Springer, Berlin, 1991.
[22] S. Chiu, A.A. Haasz, P. Franzen, J. Nucl. Mater. 218 (1995) 319.
[23] A.A. Haasz, S. Chiu, P. Franzen, J. Nucl. Mater. 220–222 (1995) 815.
[24] A.A. Haasz, J.W. Davis, J. Nucl. Mater. 175 (1990) 84.
[25] E. Vietzke, V. Philipps, Fusion Tech. 15 (1989) 108.
[26] J.W. Davis, A.A. Haasz, J. Nucl. Mater. 241–243 (1997) 37.
[27] J.W. Davis, A.A. Haasz, P.C. Stangeby, J. Nucl. Mater. 145–147 (1987) 417.